The role of spin-flip assisted or orbital mixing tunneling on transport through strongly correlated multilevel quantum dot

D. Krychowski and S. Lipiński
Institute of Molecular Physics, Polish Academy of Sciences
M. Smoluchowskiego 17, 60-179 Poznań, Poland
(Dated: March 17, 2024)

Using the slave boson Kotliar-Ruckenstein approach (SBMFA) for N level Anderson model, we compare fully symmetric SU(N) Kondo resonances occurring for spin and orbital conserving tunneling with many-body resonances for the dot with broken symmetry caused by spin, orbital or full spin-orbital mixing. As a result of interorbital or spin flip processes new interference paths emerge, which manifests in the occurrence of antibonding Dicke like and bonding Kondo like resonances. The analytical expressions for linear conductances and linear temperature thermopower coefficient for arbitrary N are found.

PACS numbers: 72.15.Qm, 73.23.-b, 73.50.Lw

I. INTRODUCTION

The growing interest in the fundamental many-body phenomenon - Kondo effect is stimulated not only by the purely cognitive purposes, but also by a rich of potential applications in quantum electronics. The spin SU(2) Kondo effect was first observed on a nanoscopic scale in semiconductor quantum dots (QD) [1]. The SU(N) Kondo physics with $N = 4$ is experimentally realized in carbon nanotubes [2] and double QDs [3]. Suggestions for realizations of SU(N) with $N = 3$ can be found e.g. in [4, 5], $N = 6$ in [6] and $N = 12$ in [7]. In this article we examine the impact of spin or orbital pseudospin flip processes associated with tunneling on many-body resonances and present how this is reflected in transport properties.

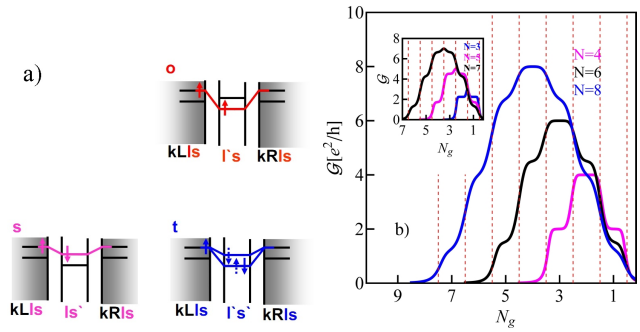

FIG. 1: (Color online) Schematic view of orbital (o), spin (s) and total (t) electrode mixing processes. (b) Conductance in the absence of mixing (nm, $\nu = 0$) as a function of dimensionless gate voltage N_g for even N (main picture) and odd N (inset), $\Gamma = 0.01$.

II. MODEL AND FORMALISM

We consider multiorbital quantum dot or a set of QDs described by generalized N-orbital Anderson model:

$$\mathcal{H} = \mathcal{H}_d + \mathcal{H}_c + \mathcal{H}^{dir}_{d-c} + \mathcal{H}^{mix}_{d-c} \tag{1}$$

where $\mathcal{H}_d = \sum_{ls} E_d n_{ls} + \mathcal{U} \sum_{l\neq l' ss'} (n_{l\uparrow} n_{l\downarrow} + n_{ls} n_{l's'})$ is hamiltonian of the dot with single- particle energy E_d and Coulomb interaction ($\mathcal{U}$), $\mathcal{H}_c = \sum_{k\alpha ls} E_k n_{k\alpha ls}$ describes electrodes ($\alpha = L, R$). $\mathcal{H}^{dir}_{d-c}$ represents direct tunneling processes $\mathcal{H}^{dir}_{d-c} = \mathcal{V} \sum_{k\alpha ls} (c^\dagger_{k\alpha ls} d_{ls} + h.c.)$ and the mixing term reads $\mathcal{H}^{mix}_{d-c} = \mathcal{V}' \sum_{k\alpha lsl's'} (c^\dagger_{k\alpha ls} d_{l's'} + h.c.)$ where $s' \neq s$ or $l' \neq l$. In general the direct hopping integral $\mathcal{V}$ differs from mixing hopping integral $\mathcal{V}'$. The degree of mixing will be characterized by parameter $\nu = \mathcal{V}'/\mathcal{V}$, $0 \leq \nu \leq 1$.

In the present paper we compare transport properties of the fully symmetric SU(N) systems (nm-no mixing between the channels) ($\mathcal{V}' = 0$) with transport in the following cases explained on Fig. 1a: tunneling conserving only spin - orbital mixing (o-different orbital channels are mixed), $(\alpha kls) \leftrightarrow (l's)$ where $l' \neq l$, tunneling conserving only orbital quantum numbers - spin mixing (s), $(\alpha kls) \leftrightarrow (l, -s)$ and the case when mixing occurs both in the spin and orbital sectors (t-mixing of all channels) i.e. tunneling of (o) and (s) types enriched by additional processes $(\alpha kls) \leftrightarrow (l', -s)$, where $l' \neq l$. To analyze correlation effects, we use finite $\mathcal{U}$ slave boson mean field approach (SBMFA) of Kotliar and Ruckenstein (for the details of the method see e.g.[5]). In this approach the effect of Coulomb interactions is effectively replaced by the interaction of quasiparticles (fermions) with auxiliary bosons, which project the state space onto subspaces of different occupation numbers. In MFA it leads to the picture of noninteracting quasiparticles in boson fields. The effective resonant line narrowing factors z_{ls} expressed through mean values of boson operators and correlation induced shifts of the dot energies λ_{ls} are found in self consistent SBMFA equations (minimum of the free energy [5]). As results from symmetry z_{ls} and λ_{ls} for nm, t and o^{even} cases, are equal for all (ls), $z \equiv z_{ls}$, $\lambda \equiv \lambda_{ls}$ (the introduced top notes inform whether an even or odd number of channels are involved in mixing). For the cases o^{odd} and s^{odd}

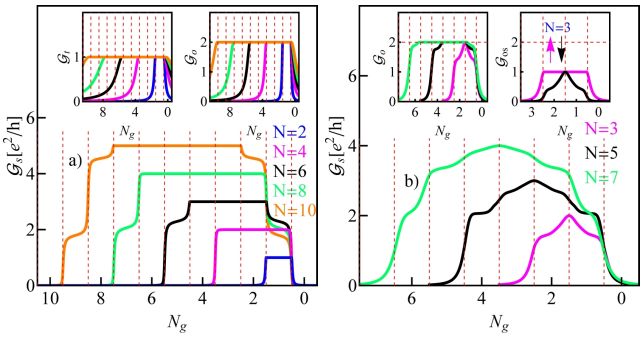

FIG. 2: (Color online) The total conductances for $\nu = 1$ versus gate voltage: a) for the spin mixing (s^{even} for even N), left and right insets present the similar conductance curves for (t) and (o^{even}) respectively. b) Total conductances for odd number of dot states (s^{odd} - main picture, o^{odd} left inset). The right inset shows spin up and spin down contributions to the conductance for $N = 3$.

there are two values for z and λ: $z_+ \equiv z_{l+}, z_- \equiv z_{l-}$ ($\lambda_+ \equiv \lambda_{l+}, \lambda_- \equiv \lambda_{l-}$) ($o^{odd}$) and for s^{odd}: $z_1 = z_{ls}$ (where $l = 1, ..(N-1)/2$) and $z_2 = z_{(N+1)/2+}$. Analogously, there are also two values of λ: $\lambda_{1(2)}$. Mixing of electrode channels $\mathcal{H}^{mix}_{d-c}$ results in the dot states ls being mixed. We will number the new basis of independent states on the dot (bonding, antibonding) with the index m, $m = 1, ...N$. In this basis conduction ($\mathcal{G}$) and thermoelectric power ($\mathcal{S}$) can be expressed by transport coefficients as follows: $\mathcal{G} = \sum_m \mathcal{G}_m = \sum_m (e^2/h)\mathcal{L}_{m0}/T$, $\mathcal{S} = \sum_m \mathcal{S}_m = \sum_m (-k_B/e)\mathcal{L}_{m1}/(T\sum_{m'} \mathcal{L}_{m'0})$, where $\mathcal{L}_{mn=0,1} = \sum_\alpha \int_{-\infty}^{+\infty} (E-\mu_\alpha)^n f_\alpha(E)\mathcal{T}_m(E)dE$. $f_\alpha(E)$ are the Fermi distribution functions of electrodes and $\mu_\alpha = \pm V_{sd}/2$. The m-th channel contribution to the transmission reads $\mathcal{T}_m(E) = (\Lambda_m\Delta_m)/((E-E_m)^2+\Delta_m^2)$, where Δ_m and $E_m = E_d + \lambda_m$ are width and position of many-body resonance. The explicit expressions for Λ_m and Δ_m are given in Sec. 3.

III. RESULTS

One can decompose the total linear conductance into separate contributions from bonding (B), antibonding (A) and unmixed states (C). State (C) indexed by quantum numbers of isolated dot (ls) occurs only for odd values of N. In the following we will choose as (C) state ((N + 1)/2,+). In the limit of $V_{sd} \to 0$, $T \to 0$ conductance reads:

$$\mathcal{G}_m = \frac{e^2}{h} \lim_{T,V_{sd}\to 0} \frac{\sum_\alpha \frac{\Lambda_m}{4\pi} Re\left[\Psi_1\left(\frac{1}{2} + \frac{E_m - \mu_\alpha + i\Delta_m}{2\pi i T}\right)\right]}{T}$$
$$\approx \frac{e^2}{h}\frac{\Lambda_m\Delta_m}{T^2_{mK}} \qquad (2)$$

where Ψ_1 is hypergeometric trigamma function. T^2_{mK} denotes characteristic resonance temperature calculated in SBMFA, which can be written as $T^2_{mK} = E^2_m + \Delta^2_m$ [8]. Amplitudes Λ_m and resonance widths Δ_m depend on the type of mixing. In the case (t) there occur $(N-1)$ dot antibonding states (A) and one bonding state (B) and then $\Lambda_A = (N-1)\Delta_A = (N-1)(\nu-1)^2\Gamma z^2$ and $\Lambda_B = \Delta_B = ((N-1)\nu+1)^2\Gamma z^2$. $\Gamma = (2\pi\mathcal{V}^2)/2D$, where D is the bandwidth. For orbital mixing (o) the situations with an even and an odd number of dot states should be distinguished. For o^{even} the amplitudes are given by $\Lambda_A = 2(N/2-1)\Delta_A = 2(N/2-1)(\nu-1)^2\Gamma z^2$

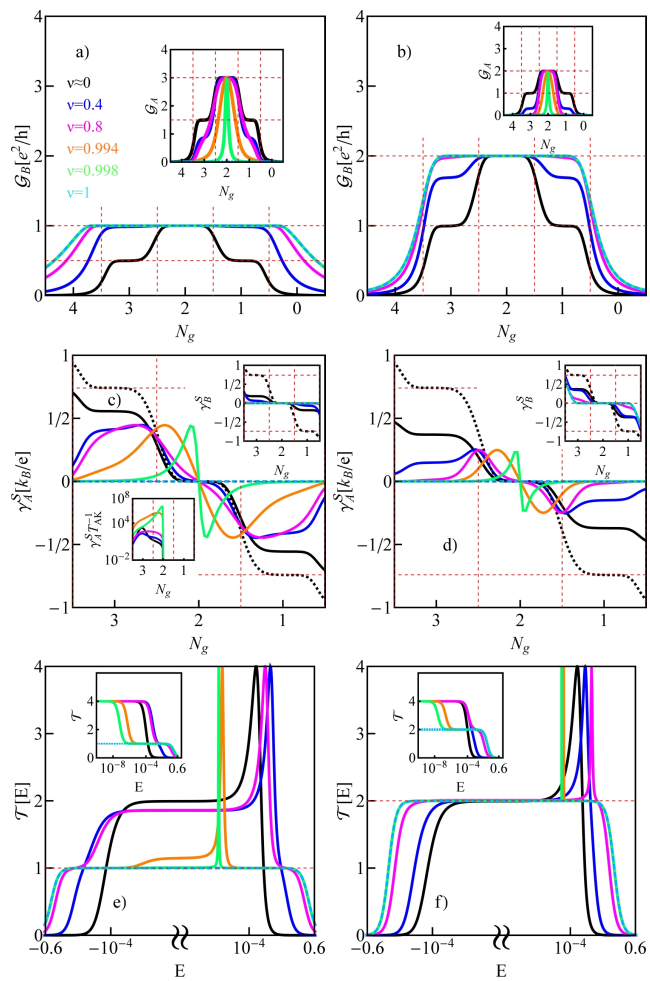

FIG. 3: (Color online) Conductances for different mixing parameters ν, $N = 4$. a) Bonding state contribution to the conductance (main picture) vs. N_g for (t) type mixing for different parameters ν and corresponding antibonding contributions (inset). b) Conductance from B states and in the inset from A states for (s^{even}) or (o^{even}) cases. Figs. c,d present linear thermoelectric coefficients corresponding to antibonding and in the upper insets for bonding states for the cases of total (c) and spin mixing -(d). The left lower inset of (c) shows the example of giant thermopower (the black dotted curve is the reference line for SU(4) symmetry). e,f) Corresponding total transmission lines for case t and s^{even} correspondingly for $N_g = 1$ and in the insets for $N_g = 2$, $\Gamma = 0.03$.

$(\Lambda_B = 2\Delta_B = 2(\nu+1)^2\Gamma z^2)$ and for case o^{odd}: $\Lambda_{A_\pm} = (N_\pm - 1)\Delta_{A_\pm} = (N_\pm - 1)(\nu-1)^2\Gamma z_\pm^2$ and $\Lambda_{B_\pm} = \Delta_{B_\pm} = ((N_\pm - 1)\nu + 1)^2\Gamma z_\pm^2$. For the spin mixing, one also has to distinguish between the case of even or odd N. For s^{even} case $\Lambda_A = (N/2)\Delta_A = (N/2)(\nu-1)^2\Gamma z^2$ and $\Lambda_B = (N/2)\Delta_B = (N/2)(\nu+1)^2\Gamma z^2$. For s^{odd}: $\Lambda_A = ((N_1-1)/2)\Delta_A = ((N_1-1)/2)(\nu-1)^2\Gamma z_1^2$, $\Lambda_B = ((N_1-1)/2)\Delta_B = ((N_1-1)/2)(\nu+1)^2\Gamma z_1^2$ and the amplitude of the unmixed state $\Lambda_C = \Gamma z_2^2$.

In the limit $V_{sd} \to 0$ and $T \to 0$ the linear temperature coefficient of thermopower defined by $\gamma_m^{\mathcal{S}} = \frac{\mathcal{S}_m T_{mK}}{2\pi T}$ takes the value:

$$\gamma_m^{\mathcal{S}} = \lim_{T,V_{sd}\to 0} \frac{-k_B T_{mK} Im\left[\sum_\alpha \frac{\Lambda_m(E_m-\mu_\alpha+i\Delta_m)}{4\pi i}\Psi_1\left(\frac{1}{2}+\frac{E_m-\mu_\alpha+i\Delta_m}{2\pi i T}\right)\right]}{e2\pi T^2\sum_{\alpha m'}\frac{\Lambda_{m'}}{4\pi}Re\left[\Psi_1\left(\frac{1}{2}+\frac{E_{m'}-\mu_\alpha+i\Delta_{m'}}{2\pi i T}\right)\right]} \approx \frac{-k_B\pi E_m\Delta_m\Lambda_m\prod_{n\neq m}^{N-1}T_{nK}^2}{3eT_{mK}\sum_m^N\Delta_m\Lambda_m\prod_{n\neq m}^{N-1}T_{nK}^2} \quad (3)$$

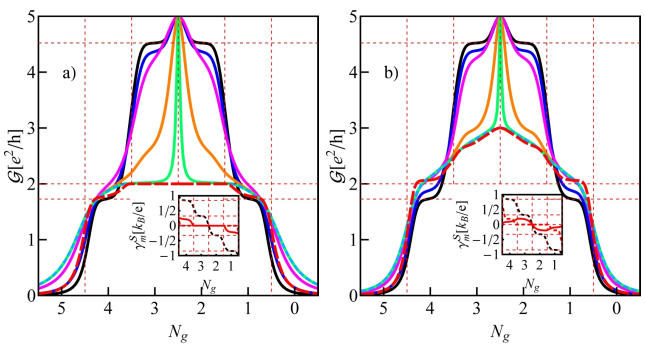

FIG. 4: (Color online) Conductances for the same choice of mixing parameters as in Fig. 3, here for $N = 5$: a) orbital mixing (o^{odd}), b) spin mixing (s^{odd}), $\Gamma = 0.03$. The red solid lines are drawn as the references (case $\nu = 1, \Gamma = 0.02$). Insets present $\gamma_m^{\mathcal{S}}$ for orbital and spin mixing respectively ($\nu = 0$ black line, $\nu = 1$ red lines: for left inset $m = B2$ (solid), $m = B1$ (dashed), and for right $m = C$ solid, $m = B$ dashed.

where $\mathcal{S}_m$ denotes the electron contribution to the thermopower from state m. For $\nu = 0$ the above formula takes the form $\gamma^{\mathcal{S}} = \gamma_A^{\mathcal{S}} + \gamma_B^{\mathcal{S}} = -(k_B/e)(\pi/3)E_N/T_{NK}$ where E_N and T_{NK} are position of the resonance and Kondo temperature for SU(N) respectively. We pay special attention to $\gamma^{\mathcal{S}}$ coefficient, because this quantity similar to the conductance has distinct plateaus in the range of strong Kondo correlations (the examples for SU(4) are shown on Figs. 3c,d). From the conductivity measurements one gets information about Kondo temperature, while $\gamma^{\mathcal{S}}$ coefficient supplements information about resonance by specifying energy location of the resonance. Using SBMFA expressions on E_N and T_{NK}: $E_N = \Delta_N cot(\pi n)$ and $T_{NK} = \Delta_N/|sin(\pi n)|$ [8], $\gamma^{\mathcal{S}}$ can also be written in the form $\gamma^{\mathcal{S}} = -(k_B/e)(\pi/3)cos(\pi n)$, where n denotes the occupation number. For the special case of SU(4) symmetry this result has already been derived earlier in [9]. For $\nu = 1$ $\gamma^{\mathcal{S}} = \gamma_B^{\mathcal{S}} = -(k_B/e)(\pi/3)E_B/T_{BK}$ and at the point of electron-hole symmetry (e-h) ($E_d = -(3/2)\mathcal{U}$) $\gamma^{\mathcal{S}} = 0$.

The numerical results discussed below are presented with the use of energy unit $D/50 = 1$ and we take $\mathcal{U} = 3$. It is convenient to work with a dimensionless gate voltage defined by $N_g = (1/2)(1-2E_d/\mathcal{U})$. This quantity approximately describes occupation regions.

Fig. 1b shows examples of gate voltage dependencies of conductance of fully symmetric systems SU(N) ($\nu = 0$) for even number of dot states $N = 4, 6, 8$ and in the inset for odd values $N = 3, 5, 7$. Clearly seen successive plateaus are the manifestations of SU(N) Kondo effects in different occupation regions. For the currently analyzed case of no mixing, the values of conductance are dictated by Friedel sum rule $\mathcal{G} = N sin^2\left(\frac{\pi n}{N}\right)$. For even N, Kondo resonance at the e-h symmetry point locates at the Fermi level and the corresponding Kondo temperature is the lowest of the entire occupation range and conductance is the highest and takes the value $N(e^2/h)$. Maximum of conductance visible for odd N places also on the e-h symmetry point and has a value $N(e^2/h)$, but in this case it locates at the border of the Coulomb blockade.

Fig. 2 presents conductances for the opposite case of full mixing ($\nu = 1$) of different types. Fig. 2a concerns s^{even} mixing. As a result of spin mixing one bonding state (B) and one antibonding state (B) are formed in each of the $N/2$ orbital sectors. For $\nu = 1$ only the first type of states contributes to the conductance and therefore it takes the value e^2/h, which is the value for SU(N/2). For the special case of $N = 4$ this effect has already been described earlier in [10] as a symmetry reduction SU(4)$\to$ 2LSU(2)(two-level SU(2)). The effect discussed here is a generalization: SU(N)$\to$ (N/2)LSU(N/2). Conductances for the other two types of mixing are shown in the insets (left inset - (t) mixing, right - (o)). In the case (t), $(N-1)$ A states and one B state are formed and only the latter contributes to the conductance for $\nu = 1$. This wide resonance centered at the Fermi level is a result of joint action of cotunneling and interference processes and gives unitary contribution, equal independent of N value ($\mathcal{G} = 2(e^2/h)$). The plateau occurring in a wide range of gate potential indicates the correlative nature of this resonance. For the case o^{even} in each of spin sectors $(N/2-1)$ A states are formed and one state B. Unitary contribution to the con-

ductance give two degenerate B states with opposite spins $\mathcal{G} = 2(e^2/h)$. Here we encounter also 2LSU(2) Kondo effect.

Fig. 2b illustrates the case of odd numbers N ($\nu = 1$). For s^{odd} there are $(N-1)/2$ A states and the same number of B states and additionally appears unmixed state (C). This time not only B states, but also C state contribute to the conductance. As an example we show in the right inset the partial conductances, where it is seen that B state contribution exhibits wide plateau, whereas gate dependence of C maps the shape of the output symmetry SU(3), of course with different limits of conductance. Due to the lack of mixing, state C retains the memory of the original symmetry. For the orbital mixing case (o^{odd} - left inset), the two spin sectors are not equinumerous, $(N+1)/2$ states with spin up and $(N-1)/2$ states with spin down. As a consequence, two types of bonding states and two types of antibonding states appear. In the areas $N_g \approx 1$ and $N_g \approx (N-1)$ two bonding states are nondegenerate. Lower on the energy scale gives a unitary contribution to the conductance and higher gives less than unity. With the increase of N, however, the energy difference between both states decreases and then also the latter contribution reaches the unitary limit. In other occupation areas two bonding states are degenerate and conductance is unitary. It is worth to emphasize that while in the case of 2LSU(2) resonance, partial transmissions from both orbitals are identical in the entire energy range, in the case now under discussion, the lines from both degenerate orbitals differ, they are centered on the same energy value, but their widths are different.

Figures 3 and 4 present evolution of conductance and linear temperature coefficient of thermopower with the increase of mixing. Fig. 3 shows examples for even $N(N = 4)$ and Fig. 4 for odd ($N = 5$). These cases distinctly differ, which was already evident in the limit $\nu \to 1$. As we have mentioned for even N and $\nu = 1$ only one bonding state is involved in the transport, whereas for odd N two bonding states or one bonding and one unmixed state. Fig. 3a shows partial conductance related to the bonding states ($\mathcal{G}_B$) and in the inset contribution from antibonding ($\mathcal{G}_A$). It is seen that with the increase of ν the gate dependence of $\mathcal{G}_B$ loses the shape of the output symmetry and partial conductance evolves to the unitary limit associated with the domination of the state B. The gate dependence of antibonding contribution (inset of Fig. 3a) for $\nu = 0$ starts from a shape typical for the output symmetry and gradually quenches with the increase of ν, most effectively further from the e-h symmetry point. Removal of degeneracy caused by mixing is weakest close to e-h symmetry point and in this region $\mathcal{G}_A$ maintains the value corresponding to the fully symmetrical system even for ν close to 1. Fig. 3b illustrates similar process, this time with mixing in the spin or orbital sector, which for $N = 4$ is equivalent, because spin and orbital pseudospin have the same dimension in this case. One can see, that the bonding contribution approaches value $2(e^2/h)$ due to participation of two B states and states A gradually contribute less and less to the conductance and disconnect for $\nu = 1$ (2LSU(2)[10]). Fig. 3c,d supplement information on transport properties by presentation of thermopower coefficients: bonding contribution $\gamma_B^{\mathcal{S}}$ and antibonding $\gamma_A^{\mathcal{S}}$ in the insets. Due to the centering of the bonding resonance on E_F with the increase of ν, also in $N_g \approx 2$ areas $\gamma_B^{\mathcal{S}} \to 0$ (see Fig. 3f,g illustrating evolution of transmission with the change of ν). $\gamma_A^{\mathcal{S}}$ gradually disappears in the $N_g \approx 1, 3$ regions , because A resonance itself disappears. In the region $N_g \approx 2$ the maximum of $\gamma_A^{\mathcal{S}}$ is clearly marked $\gamma_A^{\mathcal{S}} = 1/\left(1 + \frac{\Lambda_B \Delta_B T_{AK}^2}{\Lambda_A \Delta_A T_{BK}^2}\right)^2$, which is associated with narrowing of the resonance peak, for $\nu = 1$ A state sharply disconnects ($\gamma_A^{\mathcal{S}} = 0$)(insets of Figs. 3e,f). It is worth mentioning that thermopower reaches gigantic values in the point, where $\gamma_A^{\mathcal{S}}$ has its maximum (left down inset on Fig. 3c). This is a consequence of the fact that for this energy the resonance peak is extremely narrow and its distance from E_F is smaller than the width.

Figs. 4a,b illustrate evolution of conductance for $N = 5$ with the increase of mixing. For orbital mixing (Fig. 4a) conductance in the regions $N_g \approx 2, 3$ decreases from the value characteristic for SU(5) symmetry $5(5/8 + \sqrt{5}/8)(e^2/h)$ to value $2(e^2/h)$, which is dictated by the participation of two degenerate bonding states. In the regions $N_g \approx 1, 4$ conductance increases from $5(5/8 - \sqrt{5}/8)(e^2/h)$. This is caused by lifting of degeneracy of the bonding states. The energetically lower bonding state (B1) moves closer to E_F and this state makes a major contribution to the conductance (e^2/h). The second bonding state (B2) has a smaller contribution. Due to centering of B1 resonance line at the Fermi level $\gamma_{B1}^{\mathcal{S}} = 0$, while $\gamma_{B2}^{\mathcal{S}} \neq 0$(inset of Fig. 4a). For $N \to \infty$ and $\nu \to 1$ also B2 resonance line locates on Fermi level and then total conductance approaches unitary limit $2(e^2/h)$ and $\gamma_{B1}^{\mathcal{S}} = \gamma_{B2}^{\mathcal{S}} = 0$. For comparison we also present $\gamma^{\mathcal{S}}$ for the fully symmetric case SU(5) and it exhibits plateuas with the values characteristic for a given symmetry and occupation regions: $\frac{\mp\pi(\pm 1+\sqrt{5})}{12}$ (see Eq. 3). Case s^{odd} ($N = 5$) illustrated on Fig. 4b differs from the situation presented on Fig. 4a in the presence of two bonding states and one unmixed state. In the regions $N_g \approx 2, 3$ resonance lines from two bonding states center on the Fermi level for $\nu \to 1$ ($\mathcal{G}_B = 2(e^2/h)$, $\gamma_B^{\mathcal{S}} = 0$), and the line corresponding to the unmixed state C centers at E_F only at e-h symmetry point and there it contributes to the conductance ($\mathcal{G}_C = (e^2/h)$ and $\gamma_C^{\mathcal{S}} = 0$). In the regions $N_g \approx 1, N-1$ both bonding and unmixed lines are shifted from the Fermi level, which is visible in both the conductivity and γ coefficients. For $N \to \infty$ and $\nu = 1$ only bonding states contribute to the conductance in these regions.

Summarizing, in the present paper we have derived the general expressions for the linear conductance and linear temperature coefficient of thermopower for strongly correlated multilevel quantum dot in the case of spin-flip

assisted or orbital mixing tunneling and analyzed evolution of transport properties with the degree of mixing. For the fully symmetrical systems SU(N) both conductance and thermopower coefficient show in strong correlation regimes plateaus with characteristic values for a given symmetry and occupation number. In the case of full mixing, observed universal values of conductance are dictated by the number of states active in transport and this in turn depends on the type of mixing and parity of the number of states of the dot. We suggest that close to the full mixing one can expect a gigantic value of thermopower.

[1] D. Goldhaber-Gordon, H. Shtrikman, D. Mahul, D. Abuschmagder, U. Meiraev and M. A. Kastner, *Nature* **391**, 156 (1998). DOI: 10.1038/34373

[2] P. Jarillo-Herrero, J. Kong, H. S. J. van der Zant, C. Dekker, L. P. Kouwenhoven and S. De Franceschi, *Nature* **434**, 484 (2005). DOI: 10.1038/nature03422

[3] A. J. Keller, S. Amasha, I. Weymann, C. P. Moça, I. G. Rau, J. A. Katine, H. Shtrikman,G. Zaránd and D. Goldhaber-Gordon, *Nat. Phys.* **10**, 145 (2014). DOI: 10.1038/nphys2844

[4] C. P. Moca, A. Alex, J. von Delft and G. Zaránd, *Phys. Rev. B* **86**, 195128 (2012). DOI: 10.1103/PhysRevB.86.195128

[5] D. Krychowski and S. Lipiński, *Eur. Phys. J. B* **91**, 8 (2018). DOI: 10.1140/epjb/e2017-80547-y

[6] I. Kuzmenko, T. Kuzmenko, Y. Avishai and G.-B. Jo, *Phys. Rev. B* **93**, 115143 (2016). DOI: 10.1103/PhysRevB.93.115143

[7] I. Kuzmenko and Y. Avishai, *Phys. Rev. B* **89**, 195110 (2014). DOI: 10.1103/PhysRevB.89.195110

[8] P. Coleman, *Introduction to Many Body Physics* (Springer NY, 2012). DOI: 10.1017/CBO9781139020916

[9] P. Roura, L. Tosi, A. A. Aligia and P. S. Cornaglia, *Phys. Rev. B* 86, 165106 (2012). DOI: 10.1103/PhysRevB.86.165106

[10] C. A. Bússer, E. Vernek, P. Orellana, G. A. Lara, E. H. Kim, A. E. Feiguin, E. V. Anda and G. B. Martins, *Phys. Rev. B* 83, 125404 (2011). DOI: 10.1103/PhysRevB.83.125404